Our results point to the weakness in assuming, as is usually done, that the maximum value of PDI for condensation reactions in a well-mixed batch reactor is 2. Thus, if a polymerization reaction is controlled by monitoring the number average molecular weight, the resulting $\overline{M}_w$ can be widely different, depending on whether R was slightly below or above 1. Thus, for $K = 10$, if R is 0.99, $\overline{M}_n$ is 100 M_A, and $\overline{M}_w$ is 200 M_A, but if R is changed to 1.01, $\overline{M}_n$ remains the same, but $\overline{M}_w$ becomes 1 800 M_A. In this connection, it is to be noted that the maximum value attained by MPDI (and not the PDI) for all R is 2, but a modified definition of number average has to be employed to get the value of $\overline{M}_w$. Since the unreacted monomer contributes only negligibly to $\overline{M}_w$, this is almost the same as $\overline{M}_w'$. Thus, though $\overline{M}_n$ and $\overline{M}_n'$ will be widely different, the $\overline{M}_w$ and $\overline{M}_w'$ are almost equal.

When $K > 2$, another unusual feature is observed in the MWD itself. At sufficiently large but incomplete conversion, the probability $\alpha - \gamma$ of finding an unreacted A group attached to a polymer is so low that it is less than the product of the probability γ of reaction of an A group attached to a polymer and the probability $(1 - \alpha)$ of finding an unreacted B group. Hence, the weight fraction of the species of the type $(BBAA)_n$ is lower than the weight fraction of the species of the type $(BBAA)_nBB$. Thus, the weight fraction of any species containing an even number of units is less than the weight fraction of the next larger species containing one more unit, even when n is large. This disparity in the weight fractions is so large that two separate curves, one each for molecules containing even and odd number of units, may be drawn as done in Figure 8 for $K = 5$. This disparity is present, though in a decreased form, even when $\alpha \rightarrow 1$.

NOTATION

A = molar concentration of A_1A_2 or AC or AA
A_0 = initial molar concentration of A_1A_2 or AA or AC
B_0 = initial molar concentration of BB
K = k_2/k_1
k_1, k_2 = reaction rate constants of the monomer
M_A = molecular weight of A_1A_2 or AA or AC
M_B = molecular weight of BB
$\overline{M}_n$ = number average molecular weight
$\overline{M}_n'$ = number average molecular weight, excluding the monomeric contribution
$\overline{M}_w$ = weight average molecular weight
$\overline{M}_w'$ = weight average molecular weight, excluding the monomeric contribution
p_n = molar concentration of polymer having $(n + 1)$ units of A_1A_2 or AC or AA and n units of BB, the superscripts indicate the end group in case of A_1A_2
q_n = molar concentration of polymer having $(n - 1)$ units of A_1A_2 or AC or AA and n units of BB
r_n = molar concentration of polymer having n units of A_1A_2 or AC or AA and n units of BB, superscript indicates the end group in case of A_1A_2
R = A_0/B_0
t = time
α = fraction of initial B groups that reacted
β = fraction of initial A_1 groups or cyclic monomer or monomer with induced asymmetry that reacted
γ = ratio of initial A_2 groups or C groups or polymeric A groups that reacted to the initial number of the corresponding monomer molecules

LITERATURE CITED

Case, L. C., "Molecular Distributions in Polycondensations Involving Unlike Reactants. II. Linear Distributions," *J. Polymer Sci.*, **29**, 455 (1958).

Kilkson, H., "Effect of Reaction Path and Initial Distribution on Molecular Weight Distribution of Irreversible Condensation Polymers," *Ind. Eng. Chem. Fundamentals*, **3**, 281 (1964).

Lenz, R. W., *Organic Chemistry of Synthetic High Polymers*, Interscience, New York (1967).

Manuscript received August 3, 1977; revision received August 2, and accepted August 25, 1978.

Effectiveness Factors and Mass Transfer in Trickle-Bed Reactors

Rates of hydrogenation of α-methyl styrene were measured at 40.6°C and 1 atm in a recycle, trickle-bed reactor using a palladium/aluminum oxide catalyst. Data for different hydrogen concentrations in the gas and liquid feed streams suggested that except, at high liquid flow rates, on part of the outer surface of the catalyst the mass transfer limitation was very small, indicating a gas covered type of surface. A procedure was developed for evaluating effectiveness factors for the nonuniform boundary conditions existing when part of the particle surface is covered by gas.

MORDECHAY HERSKOWITZ
R. G. CARBONELL
and
J. M. SMITH
University of California
Davis, California 95616

SCOPE

In downflow of liquid and gas over a bed of catalyst particles, in the gas continuous regime (Charpentier, 1976), the outer surface of the particles may not be completely covered with liquid. Fractional coverages f, or wetting efficiencies, have been measured indirectly (for example, Colombo et al., 1976; Satterfield, 1975; Satterfield and Ozel, 1973; Schwartz et al., 1976; Morita and Smith, 1978) and found to be between about 0.6 and 1.0. If at least one limiting reactant is in the gas phase, as in hydrodesulfurization, incomplete coverage may affect the global rate and reactor design. The rate is expected to

increase as f decreases because the resistance to mass transfer of reactant from gas to particle will be less than from gas to liquid to particle. The increase will be greater for catalysts with high intrinsic rates. One can observe that the entire surface of the particles in a trickle-bed reactor is wetted. In the trickle flow regime, a fraction of the surface of a given particle is likely to be covered by a liquid film much thicker than the liquid film surrounding the remainder of the catalyst surface. The fractional coverage f has to be interpreted in terms of regions of the catalyst surface that have different mass transfer characteristics. To simplify the description, we refer to regions of the catalyst surface with thin liquid films and small liquid phase mass transfer resistance as the gas-covered side, the remainder as the liquid-covered side, and to the particle themselves as being partially covered by liquid.

The objectives of our work were twofold. We wanted first to measure global rates at operating conditions such that f would change and that this change would have a significant effect on the rate. The second objective was to develop a theory for predicting the global rate, or overall effectiveness factor, for catalyst particles partially covered by liquid. This required deriving an effectiveness factor for a nonuniform concentration on the outer surface of the particle and accounting for different mass transfer resistances on the liquid and gas covered parts of the outer surface.

Global rates were measured for the hydrogenation of α-methyl styrene on palladium/aluminum oxide catalyst particles in a batch-recycle (for the liquid phase) reactor operated at 40.6°C and 1 atm pressure and with a low (less than 10%) conversion per pass. In order to evaluate the prediction method for global rates in trickle beds, it was necessary to determine both intrinsic kinetics (the reaction is irreversible and first order) at an interior site and the intraparticle diffusivity. This was done by measuring rates as a function of flow rate for two catalyst particle sizes in an upflow, liquid-full (no gas phase) reactor. To improve the accuracy of the diffusivity, data were taken for several catalyst activities. The activity was varied by changing the amount of palladium deposited on the aluminum oxide particles. Such information was sufficient to separate the external mass transfer resistance and the intraparticle diffusion resistance from the intrinsic rate.

In the trickle-bed reactor, three types of experiments were carried out. First, hydrogen gas and liquid styrene, in equilibrium with respect to hydrogen concentration, flowed over a short bed of catalyst. The liquid rate was varied over a wide range in order to change f and to evaluate the resultant effect on the global rate. In the second type, nitrogen was used as the gas feed and styrene saturated with hydrogen as the liquid feed. These data showed the effect of the liquid covered surface on the rate by eliminating most of the reaction on the gas covered surface of the particles. Thirdly, hydrogen gas and styrene deficient in hydrogen were fed to the reactor. Results from these three kinds of experiments provided information on the effect of the gas-covered surface on the global rate.

CONCLUSIONS AND SIGNIFICANCE

For the catalyst activities employed, the liquid full data showed that both external and intraparticle mass transfer significantly affected the global rate. Effectiveness factors ranged from 0.05 to 0.6. When corrected for the reduced external surface of the porous particles, the external mass transfer coefficients agreed reasonably well with available correlations.

For high catalyst activities in liquid full operation, the global rate decreased significantly with decreasing liquid flow rates. In contrast, for the same hydrogen concentration, the rate in trickle-bed operation did not exhibit this significant decrease. This seems likely due to the increase in gas-covered surface and the resulting increase in reaction rate at the low liquid flow rates. Hence, our data suggested that global rates will be higher in trickle bed than in liquid full operation, at low liquid rates.

For the high-activity catalyst (2.5% palladium), the rate was higher at low liquid velocities than at high velocities. This suggested that f was less than unity at the low liquid velocities and that the contribution to the global rate due to the gas-covered surface was greater than that from the liquid-covered surface. Additional, striking evidence for this conclusion was provided by the trickle-bed runs with nitrogen feed and with a hydrogen deficient styrene feed. For the runs with nitrogen as the gas feed, the global rate approached zero as the liquid rate decreased. In contrast, the rate increased as the liquid rate approached zero for the runs with hydrogen-gas feed but a styrene feed low in hydrogen concentration.

The problem of an effectiveness factor for nonuniform outer surface concentrations was treated by assuming that the catalyst particle was cubic in shape. Then, by superposition theory, the linear differential mass balance with nonhomogeneous boundary conditions could be solved analytically for the intraparticle concentration as a function of the three rectangular coordinates. Combining this result with the pertinent external mass transfer coefficients on the liquid and gas covered parts of the external surface led to a prediction of the overall effectiveness factor.

The global rate data for the equilibrium feed runs were a function of but two parameters f and the mass transfer coefficient from liquid to particle, k_{Ls}. Hence, the theoretical development could be used with the equilibrium-feed data for two catalyst activities to calculate f and k_{Ls}. The fractional coverage of liquid varied from about 0.7 at $Re_c = 0.8$ to unity at $Re_c = 32$. These results fall within the rather wide range proposed by Satterfield (1975). However, a small variation in f will result in a large change in global rate in a reaction system for which mass transfer resistances are large, that is, for high-activity catalysts. The results for k_{Ls} agreed well with the directly measured mass transfer data of Goto and Smith (1975).

The method proposed for predicting the global rate in trickle beds should be applicable to any reaction system. However, in addition to a knowledge of f vs. liquid flow rate, it is necessary to know mass transfer coefficients from gas to porous particle, from gas to liquid, and from liquid to particle surface.

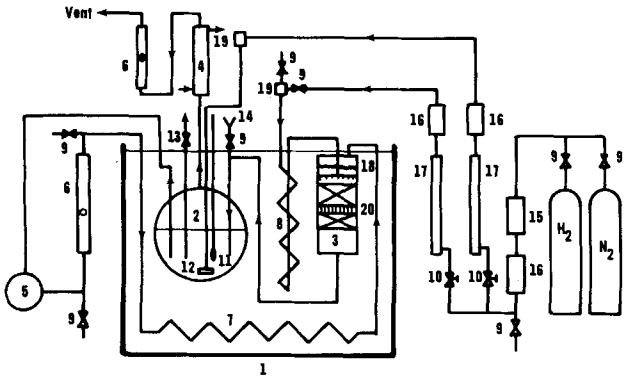

1. Thermostatic Bath
2. Styrene Reservoir
3. Trickle-Bed Reactor
4. Condenser
5. Pump
6. Rotameter
7. Liquid Preheater
8. Gas Preheater
9. Valve
10. Needle Valve
11. Thermometer
12. Dispersion Tube
13. Sample Valve
14. Funnel
15. Deoxygenator
16. Drier (Silica Gel)
17. Manometer
18. Distributor
19. Trap
20. Catalyst Bed

Fig. 1. Schematic diagram of apparatus.

The performance of trickle-bed reactors can be influenced by several unique characteristics. Of particular importance are the effects of gas-liquid-particle interphase mass transfer and the fraction of the outer surface of the catalyst particles covered by flowing liquid.

As pointed out in the review by Charpentier (1976), there are few studies of interphase mass transfer in trickle beds, in the gas continuous flow regime, with catalyst particles of conventional size and shape. Goto and Smith (1975) measured gas-liquid transfer coefficients for oxygen absorption and desorption in water. Liquid-solid transport rates were obtained for dissolution of β-naphthol particles in water. Gas-liquid coefficients were lower by almost one order of magnitude. Neither transfer rate was affected by gas velocity.

Sedricks and Kenney (1973) and Satterfield and Ozel (1973) concluded that a part of the outer surface of the catalyst particles in a trickle bed was not wetted by liquid. Colombo et al. (1976) and Morita and Smith (1978) obtained some information about how f varied with liquid flow rate Q_L. The results of these studies and others indicated that f increased with Q_L and that f approached unity at high liquid rates. However, Schwartz et al. (1976), employing a pulse-response technique concluded that $f = 0.65$ and was essentially independent of liquid rate.

Satterfield (1975) and Colombo et al. (1976) used the term contacting effectiveness to treat quantitatively the problem of incomplete liquid coverage. This effectiveness was defined as the ratio of the observed first-order rate constant (with no external diffusion resistance) in a trickle-bed reactor to the rate constant in a liquid full reactor.

The internal wetting, or fraction of the intraparticle pore volume filled with liquid, was measured by Colombo et al. (1976) and by Schwartz et al. (1976). Nearly complete wetting was reported in both instances. When the liquid wets the catalyst, the magnitude of capillary forces would lead one to expect such results. In interpreting our experimental data, which were essentially isothermal, it will be assumed that the pores are completely filled with liquid.

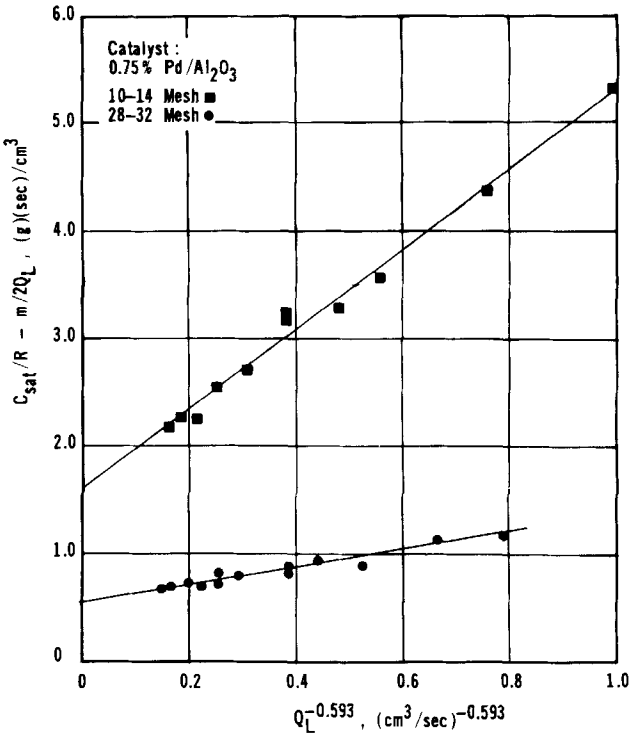

Fig. 2. Effect of liquid rate on global reaction rate (liquid-full operation).

A characteristic of the prior kinetic studies in trickle beds has been the narrow range of observed rates. An objective of our work was to operate over a range of conditions such that large differences in global rates were observed. These results should be helpful in explaining the complex effects of interphase mass transfer and partial liquid coverage of the catalyst particles.

EXPERIMENTAL

A batch-recycle reactor system (Figure 1) was used to measure reaction rates for both liquid full and trickle

Catalyst, % Pd		0.058
Shape	Cubical	
Particle mesh size	28-32	10-14
d_p or L, cm	0.0450	0.131
$(k\eta)$, cm^3/g s	0.725*	0.338*
ϕ_s or ϕ_c	3.28	9.55
η_s or η_c	0.600	0.267
k, cm^3/g s	1.25	
$D_e \times 10^4$, cm^2/s	0.90	
τ	0.79	

Catalyst, % Pd		0.75
Shape	Cubical	
Particle mesh size	28-32	10-14
d_p or L, cm	0.0450	0.131
$(k\eta)$, cm^3/g s	1.78†	0.625**
ϕ_s or ϕ_c	6.09	17.7
η_s or η_c	0.389	0.153
k, cm^3/g s	4.30	
$D_e \times 10^4$, cm^2/s	0.90	
τ	0.79	

* Reagent grade α-methyl styrene (Aldrich Chemical Co.).
† Technical grade α-methyl styrene (Dow Chemical Co.).
** Calculated from data published by Morita and Smith (1978).

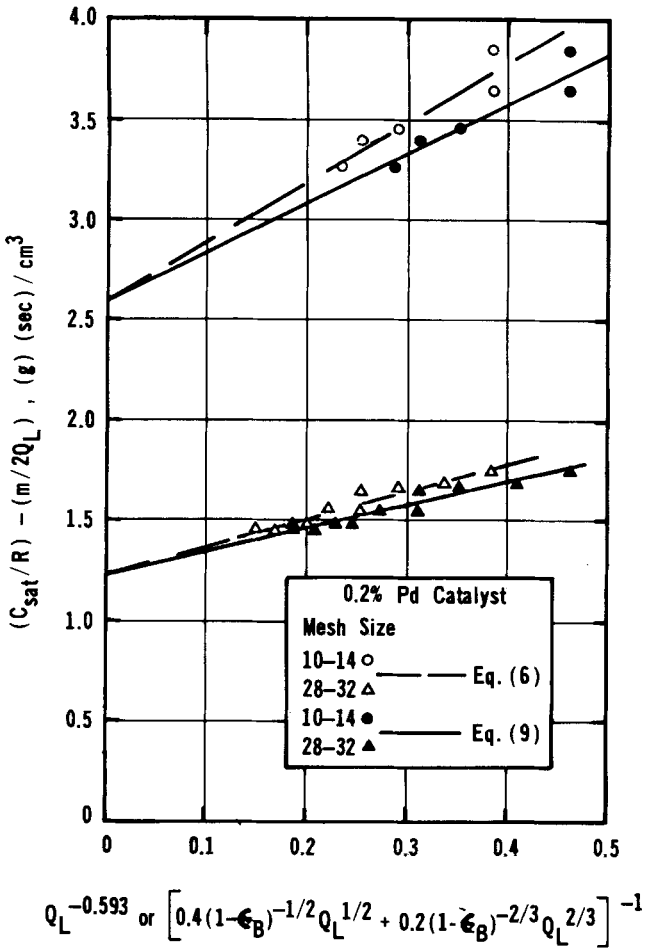

Fig. 3. Effect of mass transfer correlation on ($k\eta$), (Q_L in cm^3/sec).

operation. The amount of reaction was determined by analyzing the liquid in the system for cumene. Figure 1 shows the arrangement for the trickle bed in which gas (hydrogen or nitrogen) and α-methyl styrene (either saturated with or free of hydrogen) passed concurrently down through the reactor. The apparatus, method of operation, chemicals used, analytical methods, and catalyst preparation were nearly the same as described in earlier work (Morita and Smith, 1978). Complete details of the operating conditions and properties of the gamma-alumina particles used to prepare the catalyst are available (Herskowitz, 1978). All measurements were made at 40.6°C and 1 atm pressure. For liquid full operation, an 0.93 ID reactor was used, and for trickle-bed operation, the reactor ID was 2.54 cm. For the latter arrangement, the liquid was introduced through a distributor containing twelve 0.1 cm ID, 0.7 cm long capillary tubes uniformly spaced over the reactor cross section. According to the correlation and data of Herskowitz and Smith (1978), this arrangement gives a uniform distribution of liquid across the catalyst bed.

Two types of styrene were used: reagent grade with a stated purity of 99% and containing no cumene, and technical grade, 99.2% purity, with cumene the major contaminant. The rates of reaction were different for these two styrenes, as discussed later.

For the liquid full runs, catalysts containing 0.058, 0.20, 0.75, or 2.5 wt. % palladium (on aluminum oxide) were employed. Two catalyst particle sizes were used, 28 to 32 and 10 to 14 mesh. Liquid flow rates were varied from 4.7 to 25 cm^3/s. Rates were measured for trickle-bed operation using the 0.75 and 2.5% palladium catalyst particles of 10 to 14 mesh size. Liquid flow rates ranged from 0.25 to 10 cm^3/s and gas rates from 0.50 to 16 cm^3/s (at 25°C and 1 atm). The solubility of hydrogen in α-methyl styrene at 40.6°C and 1 atm used in analyzing the data was 2.85×10^{-6} g mole/cm^3 as determined by Herskowitz, Morita, and Smith (1978).

CALCULATION OF REACTION RATES

In all of the experiments, the concentration of cumene was nearly the same in all parts of the apparatus. During one run, the volume of all the samples withdrawn for analysis was small enough so that the total liquid volume V_{tot} changed by 1%. Under these conditions, the rate could be calculated from the batch-recycle equation

TABLE 1. RATE CONSTANTS FROM LIQUID FULL REACTOR DATA

0.20						0.50			
Spherical		Cubical		Spherical		Cubical**		Spherical**	
28-32	10-14	28-32	10-14	28-32	10-14	28-32	10-14	28-32	10-14
0.0557	0.162	0.0450	0.131	0.0557	0.162	0.0450	0.131	0.0557	0.162
0.725*	0.338*	0.806†	0.386†	0.806†	0.386†	1.32†	0.513†	1.32†	0.513†
1.02	2.97	3.61	10.5	1.13	3.29	4.95	14.4	1.55	4.51
0.664	0.229	0.570	0.245	0.626	0.273	0.457	0.183	0.507	0.206
1.11		1.51		1.36		2.84		2.55	
1.40		0.90		1.40		0.90		1.40	
0.50		0.79		0.50		0.79		0.50	

2.5									
Spherical		Cubical		Spherical		Cubical**		Spherical**	
28-32	10-14	10-14		10-14		10-14		10-14	
0.0557	0.162	0.131		0.162		0.131		0.162	
1.78†	0.625†	1.98*	1.16†	1.98*	1.16†	1.06†		1.06†	
1.92	5.58	51.7	30.2	16.1	9.57	26.6		8.79	
0.431	0.169	0.0539	0.0900	0.0610	0.108	0.109		0.110	
3.91		36.7	12.5	32.5	11.5	9.72		9.70	
1.40		0.90		1.40		0.90		1.40	
0.50		0.79		0.50		0.79		0.50	

$$R = \frac{V_{tot}}{m}\left(\frac{dC_c}{dt}\right) \tag{1}$$

During one run, the average concentration of hydrogen in the catalyst bed was nearly constant. Also, the cumene concentration increased no more than 1% during one run. Since the total conversion of styrene to cumene was always less than 5%, the styrene concentration was approximately constant and much greater than the hydrogen concentration. Accordingly, the reaction rate did not vary during one run. Graphs of the measured cumene concentration vs. time were linear, in agreement with a constant rate. The rate was calculated from the slope of such graphs using Equation (1).

Kinetics studies of the hydrogenation of α-methyl styrene with a palladium catalyst

$$C_6H_5C(CH_3) = CH_2 + H_2 \rightarrow C_6H_5CH(CH_3) - CH_3 \tag{2}$$

have been reported by Babcock (1957), Satterfield (1968), and Germain et al. (1974). Their results indicate that the reaction is first order in hydrogen and irreversible for low hydrogen and high styrene concentrations. No side reactions were observed.

ANALYSIS OF LIQUID FULL DATA

Rate Constants and Effective Diffusivity

Reaction rates calculated from the liquid full experiments were used to evaluate the intrinsic rate constant for each catalyst activity and the effective intraparticle diffusivity. This requires separation of liquid-to-particle and intraparticle mass transfer effects. For first-order kinetics, the rate may be written in terms of the surface concentration of dissolved hydrogen:

$$R = k_{Ls}a_s(C_L - C_s) = k\eta C_s \tag{3}$$

where C_L and C_s are average concentrations in the differentially operated reactor. Since the change in hydrogen concentration from entrance to exit of the reactor was small, an arithmetic average could be used for C_L; that is

$$C_L = \frac{1}{2}\left[C_{sat} + \left(C_{sat} - \frac{Rm}{Q_L}\right)\right] = C_{sat} - \frac{Rm}{2Q_L} \tag{4}$$

By eliminating C_s and C_L from Equations (3) and (4), the intrinsic rate constant k, effectiveness factor η, and liquid-to-particle mass transfer coefficient $k_{Ls}a_s$ can be expressed in terms of the rate and other known quantities:

$$\frac{1}{k\eta} + \frac{1}{k_{Ls}a_s} = \frac{C_{sat}}{R} - \frac{m}{2Q_L} \tag{5}$$

Since $k_{Ls}a_s$ depends upon liquid flow rate and $k\eta$ does not, the rate vs. Q_L data for one catalyst particle size can be used to evaluate $k\eta$. Then the data for different particle sizes are sufficient for obtaining k itself.

In order to use Equation (5) effectively, the right side should be plotted vs. a function of Q_L such that a straight line is obtained. A recent summary (Dwivedi and Upadhyay, 1977) of mass transfer data in packed beds resulted in (for $Re_s > 10$)

$$J_D = \frac{0.458}{\epsilon_B}(Re_s)^{-0.407} \tag{6}$$

where

$$J_D = \frac{k_{Ls}a_s}{a_t u_L}\left(\frac{\mu_L}{\rho_L D}\right)^{2/3} \tag{7}$$

$$Re_s = \frac{d_p u_L \rho_L}{\mu_L} \tag{8}$$

These equations suggest that $k_{Ls}a_s$ is proportional to $u_L^{0.593}$, or $Q_L^{0.593}$. Figure 2 displays typical data plotted according to Equation (5). Extrapolation of the straight lines gives an intercept equal to $1/k\eta$. The resultant $k\eta$ values for all five catalyst activities (percent palladium) and for both sizes of catalyst particles are given in Table 1. Whitaker (1972) correlated heat transfer data in packed beds as an additive function of two different powers of the Reynolds number. Adapted for mass transfer, the correlation becomes

$$J_D = \frac{0.40}{(1-\epsilon_B)^{-1/2}}(Re_s)^{-1/2} + \frac{0.20}{(1-\epsilon_B)^{-1/3}}(Re_s)^{-1/3} \tag{9}$$

Equations (7) and (9) indicates that $k_{Ls}a_s$ is proportional to $0.4(1-\epsilon_B)^{-1/2}Q_L^{1/2} + 0.2(1-\epsilon_B)^{-2/3}Q_L^{2/3}$. Experimental data plotted according to Equation (5) with this relation between $k_{Ls}a_s$ and Q_L gave $k\eta$ values within 1% of these obtained assuming $k_{Ls}a_s$ proportional to $Q_L^{0.593}$. This is illustrated in Figure 3.

In trickle-bed operation, it is likely that only part of the outer surface of the catalyst particles is covered by liquid. Hence, the hydrogen concentration may not be uniform over all of the outer surface. This leads to unsymmetrical concentration profiles within the particle, and the conventional theory for effectiveness factors is not applicable. As an approximate solution to this problem, we analyzed the trickle-bed data by assuming a cubical shape for the particle. For this shape, an analytical solution could be obtained for the effectiveness factor for discrete values of the fraction of the outer surface covered by liquid. Therefore, it was necessary to assume a cubical shape for analyzing the liquid full data to obtain k (and D_e), even though the concentration may be reasonably uniform in this case. For comparison, values of k and D_e were also obtained for spherically shaped particles.

Separate values of k and η were determined by analyzing the $k\eta$ product values for the two particle sizes. The intrinsic rate constant and D_e should be independent of particle size for a fixed catalyst activity. Hence, the values of $k\eta$ and relations $\eta = f_1(\phi)$ and $\phi = f_2(k, D_e, d_p)$ for each size provided four equations relating the four unknowns: k, D_e, and the two effectiveness factor $(\eta)_{d_{p1}}$ and $(\eta)_{d_{p2}}$. It is expected that D_e would be the same for all catalyst activities. Hence, the $k\eta$ values for all the catalysts could be used to obtain the best values of D_e and k. This was done by minimizing the square of the differences between predicted and experimental values of $k\eta$. For this purpose, data were available for two particle sizes for four catalyst activities (0.058, 0.20, 0.50, and 0.75% palladium). For the calculations based upon a spherical shaped particle, the conventional effectiveness factor relation was employed

$$\eta_s = \frac{1}{\phi_s}\left[\frac{1}{\tanh(3\phi_s)} - \frac{1}{3\phi_s}\right] \tag{10}$$

with

$$\phi_s = \frac{d_p}{6}\left(\frac{\rho_p k}{D_e}\right)^{1/2} \tag{11}$$

For the cubical shape, the following expression can be derived (Herskowitz, 1978) for the effectiveness factor in terms of cube size L and D_e and k:

$$\eta_c = 3 \sum_m \sum_n \frac{(\sin^2 \lambda_m) \sin^2 \lambda_n}{g_{mn}\lambda_m^2\lambda_n^2(\coth g_{mn})\left(\frac{1}{2} + \frac{1}{4\lambda_m}\sin 2\lambda_m\right)\left(\frac{1}{2} + \frac{1}{4\lambda_n}\sin 2\lambda_n\right)} \tag{12}$$

with

$$\left.\begin{aligned} \lambda_m &= (2m+1)\frac{\pi}{2}; \quad m = 1, 2, \\ \lambda_n &= (2n+1)\frac{\pi}{2}; \quad n = 1, 2, \\ g_{mn} &= (\lambda_m^2 + \lambda_n^2 + \phi_c^2)^{1/2} \end{aligned}\right\} \tag{13}$$

and

$$\phi_c = \frac{L}{2}\left(\frac{\rho_p k}{D_e}\right)^{1/2} \tag{14}$$

Equations (10) and (12) are for a first-order, irreversible reaction.

The results for k and D_e as calculated for both particle shapes are given in Table 1. With these values of k and D_e, experimental and calculated results for $k\eta$ differed by less than 5% for all of the catalysts. The effective diffusivity, a particularly sensitive quantity, is reduced about 35% when the cubical shape is used. In contrast, the rate constants based upon a cubical shape are within 10% of k values obtained by supposing that the particles are spherical.

Catalyst activity depends not only on palladium content but on the purity of the α-methyl styrene. This is shown in Table 1 for the 2.5% palladium catalyst where data were obtained for both grades of styrene for the larger particle size. The rate constant for the reagent grade is about threefold that obtained with the technical grade material.

The results for the 0.50% palladium catalyst and one set of data for the 2.5% palladium given in Table 1 are based upon the measurements of Morita and Smith (1978). Their measurements were made in the same type of apparatus and using the same experimental techniques. Values of $k\eta$ from their data were obtained by plotting the right side of Equation (5) vs. $Q_L^{-0.48}$. An exponent of -0.48 was chosen because it gave the most nearly linear plot of the data. However, when our more extensive results are included, there appears to be little difference in the deviation from linearity for exponents from -0.3 to -0.7. Hence, it was believed most accurate to use the correlations [Equations (6) and (9)] in extrapolating the rate data. The values of $k\eta$ (Table 1) differ by about 20% from those presented by Morita and Smith. The Morita results for the 0.5% palladium catalyst were included in evaluating D_e and k. None of the 2.5% palladium results could be used because ϕ was too large. For large ϕ, the ratio of the effectiveness factors becomes independent of k. Hence, the k values given for this catalyst were calculated from $k\eta$ using the diffusivities determined from the data for smaller values of the Thiele modulus. The k values in Table 1 for the two sets of 2.5% palladium catalyst, with the technical grade styrene, differ by 15% (spherical shape) to 30% (cubical shape). The two sets of data were obtained by different investigators and involved different batches of the 2.5% palladium catalyst. The comparison is believed to be a reasonable measure of the reproducibility of the experimental results.

Tortuosity factors calculated from the equation

$$\tau = \epsilon_p \frac{D}{D_e} \tag{15}$$

were less than unity. The value used for D, the molecular diffusivity of hydrogen in α-methyl styrene, was 1.42×10^{-4} cm^2/s at 40.6°C. This is from the experimental results obtained by Satterfield et al. (1968). Correlations for D in organic liquids, proposed by Sporka et al. (1971) and by Sovova (1976), give 2.36×10^{-4} and 1.33×10^{-4} cm^2/s, respectively. Sovova mentioned that accurate determination of the diffusivity of hydrogen in liquids is difficult because of its low solubility. Uncertainty in the value of D may explain the low values of τ, although reported tortuosity factors in liquid filled pores cover a wide range (Niiyama and Smith, 1976).

Liquid-to-Particle Mass Transfer

The $k\eta$ values determined from the intercepts in Figure 2 can be used in Equation (5) to calculate $k_{Ls}a_s$. These experimental values of liquid-to-particle mass transfer coefficients are compared with the Dwivedi and Upadhyay and the Whitaker correlations in Figure 4.

In evaluating the two Reynolds numbers, the density of α-methyl styrene at 40.6°C was taken as 0.893 g/cm^3 (Dow Chemical Co., 1955) and the viscosity as 0.00717 g/(cm)(s). The latter value was obtained by measuring the viscosity at 23.8°C in a Cannon-Fenske viscometer and extending this result to μ_L at 40.6°C using the Thomas method (Reid et al., 1977). It is convenient to make the comparison in terms of J_D as defined in Equation (7). The total external surface area (per unit mass) of the particles (assumed to be spherical) is $a_t = 6/d_p\rho_p$, and the Schmidt number for hydrogen in α-methyl styrene at 40.6°C is 56.7. For porous particles, the effective external area will be assumed to be that of the pore mouths. Hence, for comparison with nonporous particles, upon which the correlations are based, J_D from Equation (7) should be divided by ϵ_p. The experimental points in Figure 4 were obtained in this way. The lines for the Dwivedi and Upadhyay and for the Whitaker correlation are given by Equations (6) and (9).

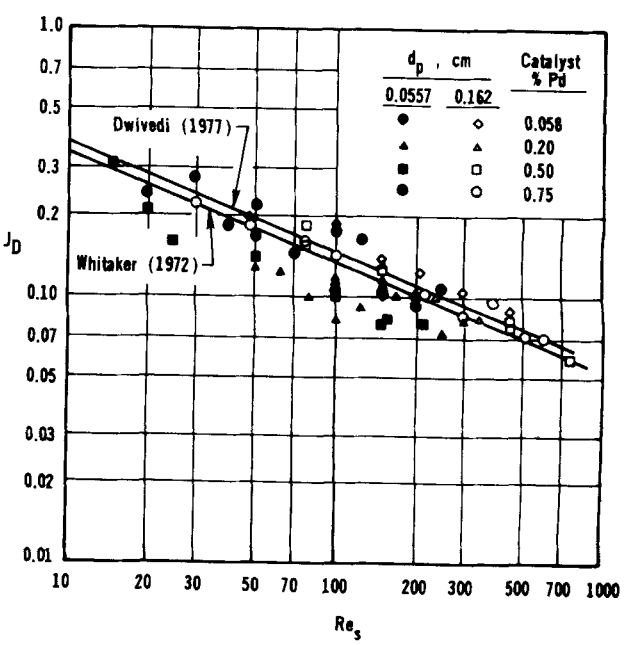

Fig. 4. Comparison of experimental and predicted J_D-factors for liquid-full operation.

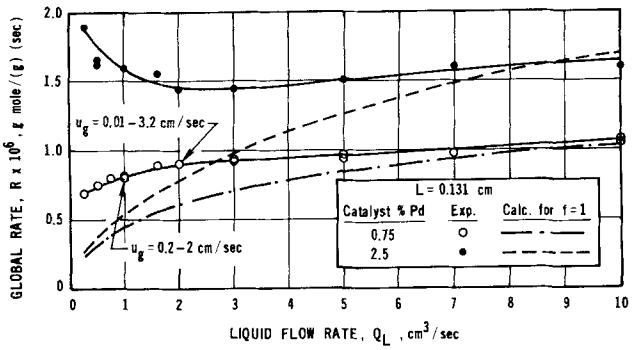

Fig. 5. Trickle-bed rates; equilibrium feed streams.

Such kinetics experiments as ours do not provide an optimum method of establishing mass transfer coefficients, and the data points in Figure 4 scatter. However, a line through the points would agree reasonably well with either correlation. Note that if the mass transfer area was not based upon the porosity of the particle, the experimental points would be about 100% below the correlation lines.

TRICKLE-BED RATE DATA

The objectives of the trickle-bed studies were to determine the effect of partial liquid coverage and interphase mass transport on the global reaction rate. To accomplish this, reaction rates were measured for three feed arrangements and for two catalyst activities for the same size particles:

1. Pure hydrogen along with styrene saturated with hydrogen was introduced to the top of the reactor. The conversion of hydrogen in the liquid leaving the short catalyst bed was always less than 10%. Hence, the average hydrogen concentration in the liquid was always within 5% of the saturation value. Such equilibrium runs were made over a wide range of liquid flow rates to augment changes in liquid coverage.

2. Pure nitrogen gas and styrene partially saturated with hydrogen were fed to the reactor. Since interphase mass transfer occurred in the top section and upstream inert packing, the gas entering the catalyst bed was not pure nitrogen, nor was the liquid saturated with hydrogen. While hydrogen was continually fed to the absorber, so much stripping of the liquid had occurred in the reactor and lines that the liquid leaving the absorber was not completely resaturated. At the highest liquid rate, the hydrogen concentration entering the reactor was 56% of saturation.

3. Pure hydrogen and styrene partially stripped of hydrogen entered the reactor. Again, because of interphase mass transfer in the inert packing and lines and because of incomplete stripping (with nitrogen) in the reservoir, the styrene feed to the reactor was not completely free of hydrogen. At the lowest flow rate the concentration was 42% of its saturation value.

Equilibrium Feed

The points in Figure 5 indicate a minimum in the measured rate at an intermediate liquid flow rate for the more active (2.5% palladium) catalyst. This suggests that the fraction of the external particle surface covered by liquid is less than unity. At low flow rates, the mass transfer coefficient from liquid to particle should decrease, causing the global rate also to decrease. Hence, the observed increase in rate cannot be explained in terms of mass transfer and reaction being controlled by the liquid covered surface. The data can be explained if part of the surface is covered by gas and if the gas-to-particle mass transfer coefficient k_{gs} is much higher than the liquid-to-particle coefficient k_{Ls}. As an order of magnitude estimate, k_{gs} was calculated from the Dwivedi and Upadhyay (1977) correlation which is applicable for two-phase packed beds. Such k_{gs} values were two orders of magnitude greater than k_{Ls} obtained from the correlation of Goto and Smith (1975), which is based upon trickle-bed mass transfer data. Further evidence for the high value for k_{gs} is that our rate measurements did not change significantly with gas flow rate at constant liquid rate (Figure 5). Additional evidence is available from the two other types of trickle-bed data. In other words, we visualize that when $f < 1$, the measured global rate has a significant contribution from the hydrogen transported directly from gas to particle. For the equilibrium runs, this reaction occurs as a result of a high k_{gs} and a small difference in hydrogen concentration in the gas and in the liquid at the pore mouths of the catalyst. Hence, as f decreases with decreasing Q_L, the rate increases. The reaction rate is unaffected by gas rate because the gas-to-particle mass transfer resistance is very small. The observed modest increase in rate at high Q_L, where $f \rightarrow 1.0$, can be explained in terms of an increase in k_{Ls} with liquid rate.

The results for the low activity catalyst (0.75% palladium) show no minimum. This is presumably due to the decreased importance of mass transfer and f; for this catalyst the rate is more nearly controlled by intrinsic kinetics and intraparticle diffusion.

For comparison with the data points in Figure 5, rates have been calculated assuming that the particle surface is fully covered by liquid ($f = 1$). The rate was evaluated from Equation (5) using the $k\eta$ value for the 0.75 and 2.5% palladium catalysts given in Table 1. Equation (5) is applicable when the hydrogen concentration in the liquid is constant. Since conversions were less than 10%, C_L is nearly constant for the equilibrium-feed experiments. The mass transfer coefficient $k_{Ls}a_s$ was estimated from the Goto and Smith (1975) correlation of trickle-bed data. For application to our porous catalysts, the correlation was corrected for the external surface available for mass transfer (that is, for the porosity):

$$\frac{k_{Ls}a_s}{D} = 90\frac{\epsilon_p}{\rho_B}\left(\frac{\rho_L\mu_L}{\mu_L}\right)^{0.6}(Sc)^{1/3} \qquad (16)$$

These computed rates are seen in Figure 4 to agree reasonably well with the data at high Q_L, where f is

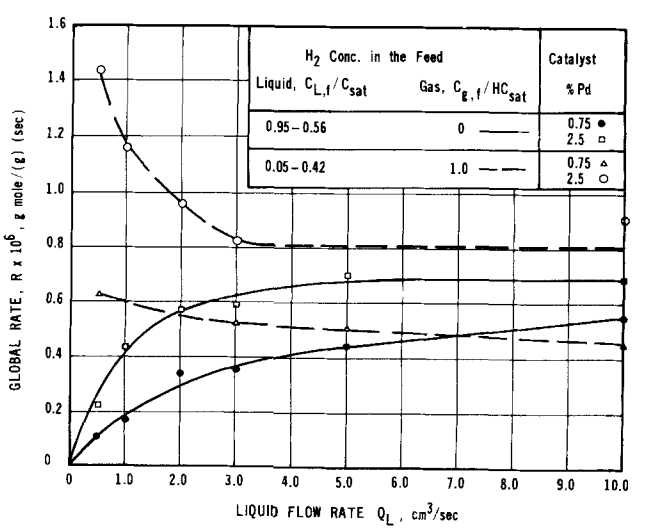

Fig. 6. Trickle-bed rates; non-equilibrium feed streams.

believed to be nearly unity. At low Q_L, the computed rates are much lower than experimental values because the contribution of the gas covered surface, with its very low mass transfer resistance, is not taken into account.

Nitrogen Feed

The rate data for a reactor feed of nitrogen gas and partially hydrogen saturated styrene are shown in the lower part of Figure 6. The rates for both catalyst activities approach zero as Q_L approaches zero because of the absence of reactant. It is instructive to compare the rates shown here for the 2.5% palladium catalyst at low Q_L, with the rates for the equilibrium feed (Figure 5). The higher values in Figure 5 provide additional evidence that the gas-covered surface can contribute significantly to the global rate. The sharp increase in rate with Q_L for the lower curves in Figure 6 is likely due to the increase in $k_{Ls}a_s$ with Q_L. The rate at the highest Q_L in Figure 6 is about one half that observed for the equilibrium feed. This is expected because the hydrogen concentration in the liquid feed at this Q_L, where $f \approx 1$, is also about half the saturation value.

Hydrogen Deficient Liquid Feed

Experimental rates for feed streams of styrene deficient in hydrogen and of pure hydrogen gas are shown by the upper two curves in Figure 6. The very high rates at low Q_L indicate that part of the catalyst surface is covered by flowing gas where the gas-to-particle mass transfer coefficient is very high. The rates at low Q_L are less than those for the equilibrium feed (Figure 5) because the hydrogen concentration in the liquid is much less than the saturation value, and, therefore, less hydrogen is transferred on the liquid covered part of the surface.

The hydrogen concentrations in the liquid entering the bed of catalyst particles were no greater in these experiments than for the experiments described previously. Yet the rate values at low Q_L are much higher for the hydrogen deficient liquid data.

TRICKLE-BED EFFECTIVENESS FACTORS

The conclusion that f is less than unity, except at high liquid rates, has also been reached in other investigations (Satterfield and Ozel, 1973; Sedricks and Kenney, 1973; Schwartz et al., 1976; Morita and Smith, 1978). If this concept is accepted, it would be helpful to be able to predict the effect of f and the several interphase mass transfer coefficients, k_{gs}, K_{gL}, k_{Ls}, on the global rate. Such results could be expressed, for a reaction for which the limiting reactant is in the gas phase, in terms of an overall effectiveness factor η_o defined by

$$R = \eta_o k C_{eq} \tag{17}$$

if Henry's law is valid, $C_{eq} = C_g/H$. Existing effectiveness factor equations are not applicable for η_o because the concentration of reactant is not uniform over the outer surface of a catalyst particle. Such nonuniformity arises because mass transfer rates on the liquid and gas covered parts of the surface are not the same.

Derivation of an appropriate effectiveness factor equation for a spherical particle would not lead to an analytical result, even for first-order kinetics. Further, the numerical solution would be cumbersome because of lack of symmetry in the angular directions. However, an analytical solution is possible for linear kinetics if the particle shape is assumed to be cubic and one or more whole faces of the cube are covered by gas or liquid. For liquid filled pores and constant effective diffusivity, the concentration within the pores can be described by a linear differential equation in rectangular coordinates. The differential equation and the appropriate boundary conditions may be solved by the separation of variables method and the superposition principle (Hildebrand, 1976), provided that entire faces of the cube are covered by gas or liquid. This means that the solution for the intraparticle concentration $C(x, y, z)$ could be obtained for only discrete number of faces of the particle covered by liquid, that is, for $f = 1/6, 1/3, 1/2 \cdots 1$. In terms of dimensionless variables, $C' = C/C_{eq}$, $X = x/(L/2)$, etc., the intraparticle concentration is described by

$$\frac{\partial^2 C'}{\partial X^2} + \frac{\partial^2 C'}{\partial Y^2} + \frac{\partial^2 C'}{\partial Z^2} = \phi_c^2 C' \tag{18}$$

where the Thiele modulus is defined by Equation (14).

Separate boundary conditions are necessary for the gas and liquid covered parts of the catalyst surface. As an illustration, suppose that the face of the cube at $x = L/2$ ($X = 1$) is covered by gas and that the other five faces are covered by liquid. For the gas covered face, the boundary condition is given by equating the mass transfer rate of reactant in the gas to that in the pores. Thus, for the face at $x = L/2$

$$\epsilon_p k_{gs}[C_{eq} - C_{x=L/2}] = D_e \left(\frac{\partial C}{\partial x}\right)_{x=L/2} \tag{19}$$

In dimensionless form this becomes

$$\frac{\partial C'}{\partial X} + \alpha_{gs} C' = \alpha_{gs} \quad \text{at} \quad X = 1 \tag{20}$$

where

$$\alpha_{gs} = \frac{\epsilon_p k_{gs}(L/2)}{D_e} \tag{21}$$

For the five liquid covered faces, the boundary condition expresses the equality of mass transfer rates from gas to liquid and liquid to solid. For example, at $z = L/2$, where

$$K_{gL}(C_{eq} - C_L) = \epsilon_p k_{Ls}(C_L - C_{z=L/2}) = D_e \left(\frac{\partial C}{\partial z}\right)_{z=L/2} \tag{22}$$

If Henry's law is valid

$$\frac{1}{K_{gL}} = \frac{1}{Hk_g} + \frac{1}{k_L} \tag{23}$$

Analogous boundary conditions would apply on the four other liquid covered faces at $X = -1$, $Y = \pm 1$, $Z = -1$. The formulation of Equation (22) supposes that the liquid rivulets in the trickle bed are thick enough that the concentration gradients near the phase boundaries occupy but a small part of the thickness. That is, the major part of the liquid has a uniform, bulk concentration C_L. The concentration C_L can be eliminated from Equations (22) and the result expressed in dimensionless form as follows:

$$\frac{\partial C'}{\partial Z} + \frac{1}{\frac{1}{\alpha_{Ls}} + \frac{1}{\alpha_{gL}}} C' = \frac{1}{\frac{1}{\alpha_{Ls}} + \frac{1}{\alpha_{gL}}} \quad \text{at} \quad Z = 1 \tag{24}$$

where

$$\alpha_{gL} = \frac{K_{gL} L/2}{D_e} \tag{25}$$

and

$$\alpha_{Ls} = \epsilon_p \frac{k_{Ls}(L/2)}{D_e} \tag{26}$$

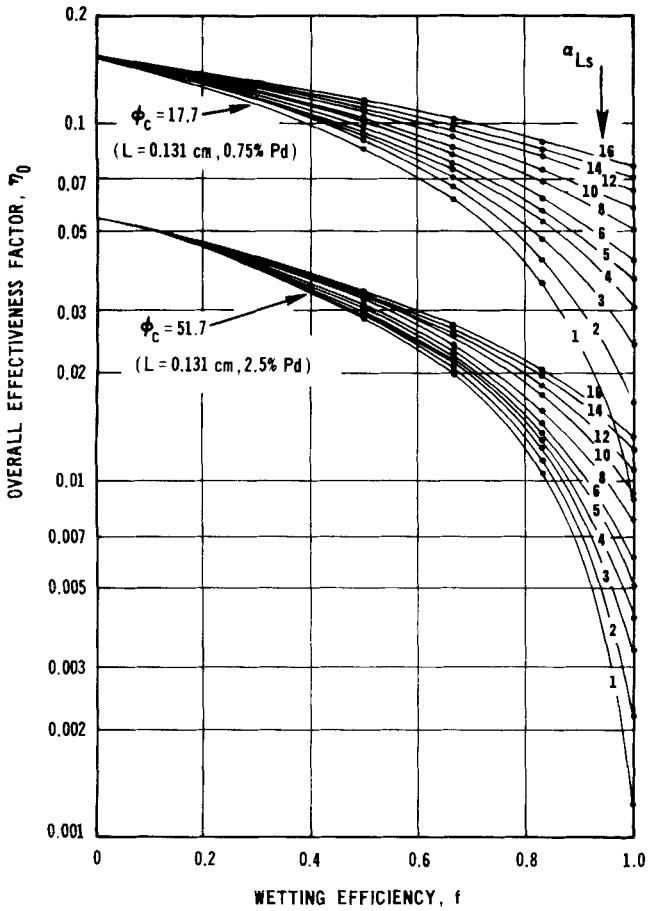

Fig. 7. Overall effectiveness factor for trickle-bed operation for $\alpha_{gs} \to \infty$ and $C_L = C_{sat}$.

Equation (18) and boundary conditions (20) and (24) can be solved by converting the five equations of the form of Equation (20) to homogeneous boundary conditions. The principle of superposition is used to add the effects of the actual nonhomogeneous form of Equation (20). The solution gives $C'(X, Y, Z)$ for $f = 5/6$. The next step is to calculate the effectiveness factor from its definition. In terms of pore-mouth concentration gradients, the result is

$$\eta_o = \frac{R}{kC_{eq}} = \frac{D_e \int_{-L/2}^{L/2}\int_{-L/2}^{L/2}\left[\left(\frac{\partial C}{\partial x}\right)_{x=L/2} - \left(\frac{\partial C}{\partial x}\right)_{x=-L/2}\right] dydz}{L^3 kC_{eq}} + \frac{D_e \int_{-L/2}^{L/2}\int_{-L/2}^{L/2}\left[\left(\frac{\partial C}{\partial y}\right)_{y=L/2} - \left(\frac{\partial C}{\partial y}\right)_{y=-L/2}\right] dxdz}{L^3 kC_{eq}} + \frac{D_e \int_{-L/2}^{L/2}\int_{-L/2}^{L/2}\left[\left(\frac{\partial C}{\partial z}\right)_{z=L/2} - \left(\frac{\partial C}{\partial z}\right)_{z=-L/2}\right] dxdy}{L^3 kC_{eq}} \quad (27)$$

Converting Equation (27) to dimensionless form and using the solution $C'(X, Y, Z)$ gives an expression that can be solved for η_o. The result applies for $f = 5/6$ and is quite lengthy. It is given in the appendix [Equation (A1)]. Equation (A1) is a function of k (through ϕ_c) and the three mass transfer coefficients involved in the definitions of α_{gs}, α_{gL}, and α_{Ls}.

Solutions for the other values of f, 4/6, 3/6, etc., can be obtained by again applying superposition theory. These solutions are available (Herskowitz, 1978). There are two ways of considering $f = 2/6$ and 4/6. Two sides of the cube covered with liquid may be taken parallel or perpendicular to each other. This gives either symmetric or unsymmetric boundary conditions and leads to solutions different in form. However, the numerical values of η_o are nearly the same (within 1%) for the two cases.

Figure 7 shows predicted η_o for the particular case of $k_{gs} \approx \infty$ ($\alpha_{gs} \approx \infty$), $C_{eq} \approx C_L$, and for $\phi = 17.7$ and $\phi = 51.7$. These conditions apply for the equilibrium feed runs; the Thiele moduli correspond to k values for the $L = 0.131$ cm particles of 0.75 and 2.5% palladium catalysts, as shown in Table 1. The points for the seven discrete values of f form smooth curves.

Figure 7 shows that the overall effectiveness factor is sensitive to the fraction of the surface covered by liquid when this fraction is large. This sensitivity is due to the negligible mass transfer resistance from gas to solid so that as f increases there will be less surface and less reaction arising from the gas covered part of the particle. The effect is increased as the mass transfer coefficient on the liquid covered surface α_{Ls} decreases, since mass transfer through the liquid covered surface also decreases. As expected, η_o is less for the more active catalyst (larger ϕ_c).

It seems that in trickle-bed reactors k_{gs} will be much larger than k_{Ls}. For this situation, the strong dependency of η_o on f, illustrated in Figure 7, is likely to occur. In any event, the theory proposed in this section offers a method for predicting the global rate for any values of the three mass transfer coefficients. The theory is applied in the next section to our trickle-bed data to obtain information about f and some of the mass transfer coefficients.

WETTING EFFICIENCY (f) AND LIQUID-PARTICLE MASS TRANSFER

For our data with gas and liquid feed streams in equilibrium, the liquid is saturated with pure hydrogen. In this case, the boundary condition on the liquid covered surface becomes, instead of Equation (22)

$$\epsilon_p k_{Ls}(C_{sat} - C_{z=L/2}) = D_e\left(\frac{\partial C}{\partial z}\right)_{z=L/2} \quad (28)$$

or, in dimensionless form

$$\frac{\partial C'}{\partial Z} + \alpha_{Ls}C' = \alpha_{Ls} \quad (29)$$

Now, the solution for η_o is not a function of K_{gL} (or α_{gL}). The result can be obtained from Equation (A1) by taking $\alpha_{gLs} = \alpha_{Ls}$. Since k_{gs} has been shown to be much larger than k_{Ls}, the mass transfer resistance from gas to particle can be neglected; that is, $\alpha_{gs} \to \infty$. Then $\eta_o = F(f, \alpha_{Ls}, \phi_c)$. Figure 7 shows this function for the two values of ϕ_c (two catalyst activities) for which equilibrium feed data were obtained.

The rate data in Figure 5 and the curves in Figure 7 can be used to evaluate f and α_{Ls} at each liquid flow rate. Thus, at any liquid rate, η_o can be calculated for each catalyst from Equation (17). These values of η_o are used in Figure 7 to find f and α_{Ls}. These two quantities should be independent of catalyst activity (for the same particle size). Hence, the two sets of curves in Figure 7, one for each catalyst, provide two relations which can be solved for f and α_{as}. A trial and error procedure can be avoided by cross plotting the curves in Figure 7 as η_o

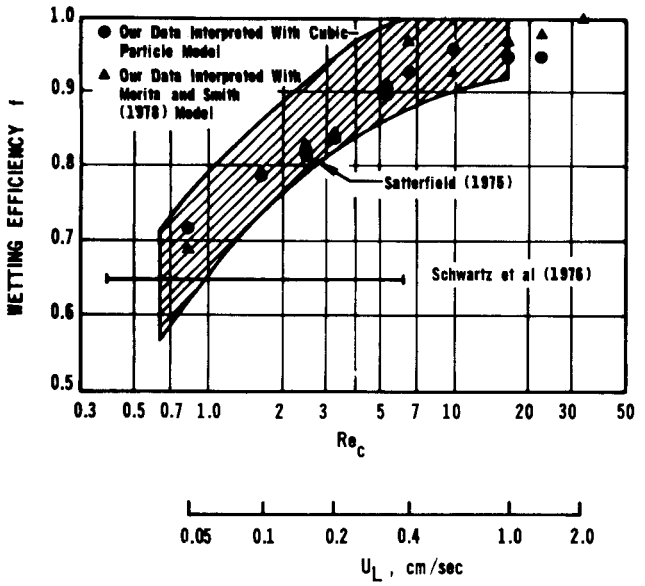

Fig. 8. Wetting efficiency in trickle-bed reactors.

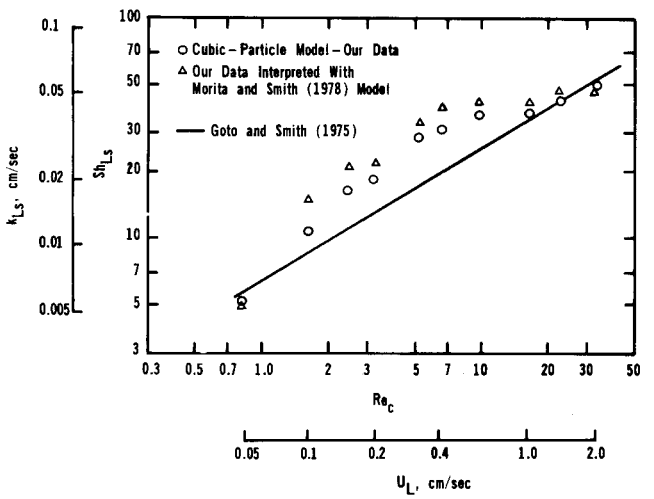

Fig. 9. Liquid-solid mass transfer in trickle-bed operation.

for one catalyst vs. η_o for the other, with α_{Ls} and f as parameters.

The circular data points in Figure 8 show f values calculated in this way using the rate data in Figure 5. The liquid coverage is complete at $u_L = 2$ cm/s and decreases to 0.7 when u_L falls to 0.05 cm/s. The shaded region was proposed by Satterfield (1975), and our results fall within his predictions. Also shown are the values of f calculated using our rate data and the model proposed by Morita and Smith (1978). Their model is a more approximate, simpler approach, based upon adding contributions to the rate from the liquid and gas covered parts of the catalyst particle. The model neglects all mass transfer resistances except from liquid to particle and assumes that the conventional expression for η, based upon uniform surface concentration, is applicable. In analyzing their own experimental results with their model, Morita and Smith found f to be about 0.89 and independent of liquid rate. However, we believe our method of treating the experimental data, particularly the extrapolation to obtain $k\eta$ (Figure 2) and the separation of k from $k\eta$, is more accurate.

From tracer experiments, Schwartz et al. (1976) found $f = 0.66$, independent of liquid rate. Columbo et al. (1976) reported values of f that are within the range proposed by Satterfield.

In summary, it seems that f has values that will, in most circumstances, fall within the shaded zone in Figure 8. Since f has a limited range, perhaps more important than the value of f is its effect on the rate. At a liquid rate corresponding to $u_L = 0.2$ cm/s, our data give $f = 0.84$. If instead, $f = 0.94$ (near the upper end of the shaded zone in Figure 8), the global rate for the 2.5% palladium catalyst would decrease by 40%. For this particular case, the rate is rather sensitive to f. Conversely, the sensitivity of f to the interpretation of experimental rate data is low. For example, if the effective diffusivity is taken to be 40% higher than the value of 0.90×10^{-4} cm^2/s (Table 1), f changes by less than 2% and α_{Ls} by less than 10%.

The α_{Ls} values calculated from the equilibrium-feed runs and Figure 7 were converted to Sh_{Ls} using Equation (26) and $Sh_{Ls} = k_{Ls}L/D$. The results are given in Figure 9. The line in Figure 9 represents the Goto and Smith correlation modified to be applicable for porous particles; that is k_{Ls} was calculated from Equation (16) and then used to evaluate Sh_{Ls}. The agreement is better than expected, since Equation (16) is based upon mass transfer data for nonporous particles, while the data points represent extensive analysis of reaction rate data through the theory represented in Figure 7. Also shown in Figure 9 are values calculated from the Morita and Smith (1978) model. These results are about 25% higher.

In the nonequilibrium experiments for a gas feed of nitrogen and for hydrogen deficient liquid feed, mass transfer from gas to liquid was significant because the concentration difference between phases was large. In principle, it is possible to evaluate K_{gL} from such data. Attempts to do this were not very successful because the extent of mass transfer in the bed of inert particles, upstream from the catalyst, was uncertain. This meant that the hydrogen concentrations in the gas and liquid entering the catalyst bed itself were not equal to the measured concentrations in the reactor feed.

ACKNOWLEDGMENT

The National Science Foundation through Grant ENG 76-01153 provided financial assistance for this research. Also acknowledged are the Fellowships of the University of California. The chemicals were supplied by Dow Chemical Company and United Catalysts, Inc.

NOTATION

a_t = total external area per unit mass of catalyst, cm^2/g
a_s = effective liquid-particle mass transfer area per unit mass of catalyst, cm^2/g
C = concentration of reactant in the liquid filled pores, mole/cm^3
C_L = concentration of reactant in the bulk liquid, moles/cm^3
C_{sat} = concentration of hydrogen in the liquid in equilibrium with pure reactant gas, moles/cm^3
C' = dimensionless concentration, C/C_{eq}
C_{eq} = concentration of gaseous reactant in the liquid in equilibrium with the gas, g mole/cm^3
D = molecular diffusivity of hydrogen in α-methyl styrene, cm^2/s
D_e = effective diffusivity of hydrogen in liquid filled pores, cm^2/s
d_p = equivalent spherical diameter of catalyst particle, cm
f = wetting efficiency; fraction of external surface of catalyst particle covered by liquid

H = Henry's law constant, (cm³ of liquid)/(cm³ of gas)
J_D = mass transfer factor, defined by Equation (7)
K_{gL} = overall gas-liquid mass transfer coefficient, cm/s
k = intrinsic, first-order rate constant, cm³/(g)(s)
k_{gs} = gas-solid mass transfer coefficient, based on the effective mass transfer area, cm/s
k_L = gas-liquid mass transfer coefficient on the liquid side of the interface, cm/s
k_g = gas-liquid mass transfer coefficient on the gas side of the interface, cm/s
k_{Ls} = liquid-solid mass transfer coefficient, for both liquid full operation and trickle-bed operation, based on the effective mass transfer area, cm/s
L = equivalent length of cubical catalyst particle, cm
m = mass of catalyst in reactor, g
Q_L = liquid flow rate
Re_s = Reynolds number, $d_p\rho_L u_L/\mu_L$, for spherical shape
Re_c = Reynolds number, $L\rho_L u_L/\mu_L$, for cubical shape
S_c = Schmidt number, $\mu_L/\rho_L D$
Sh_{Ls} = Sherwood number, $k_{Ls}L/D$
Q_L = liquid flow rate, cm³/s
R = global rate of reaction, g mole/(g)(s)
t = time, s
u = superficial velocity, cm/s
V_{tot} = total volume of liquid in reaction system, cm³
x, y, z = rectangular coordinates
X, Y, Z = dimensionless rectangular Cartesian coordinates

Greek Letters

α_{gs} = dimensionless gas-solid mass transfer coefficient, gas covered side of the particle, $\epsilon_p k_{gs}(L/2)/D_e$
α_{gL} = dimensionless gas-liquid mass transfer coefficient, $K_{gL}(L/2)/D_e$
α_{Ls} = dimensionless liquid-solid mass transfer coefficient, liquid covered side of the particle, $\epsilon_p k_{Ls}(L/2)/D_e$
α_{gLs} = dimensionless gas-liquid-solid mass transfer defined by Equation (A2)
ϵ_B = interparticle void fraction in reactor
ϵ_p = porosity of particles
η_c = effectiveness factor for cubic particle shape with uniform surface concentration, Equation (12)
η_s = effectiveness factor for spherical particle shape with uniform surface concentration, Equation (10)
η_o = overall effectiveness factor for nonuniform surface concentration defined by Equation (17)
μ = viscosity, g/(cm)(s)
ρ = density, g/cm³
ρ_B = bulk density of particles in bed, g/(cm³ of bed)
τ = tortuosity factor
ϕ_c = Thiele modulus for cubic shape, defined by Equation (14)
ϕ_s = Thiele modulus for spherical shape, defined by Equation (11)

Subscripts

c = cumene
f = feed
g = gas
L = liquid
p = particle
s = external surface of catalyst

LITERATURE CITED

Babcock, B. D., G. T. Mejdell, and O. A. Hougen, "Catalyzed Gas-Liquid Reactions in Trickling-bed Reactors," *AIChE J.*, 3, 366 (1957).

Charpentier, J. C., "Recent Progress in Two-Phase Gas-Liquid Mass Transfer in Packed Beds," *Chem. Eng. J.*, **11**, 161 (1976).

Colombo, A. J., G. Baldi, and S. Sicardi, "Solid-Liquid Contacting Efficiency in Trickle Bed Reactors," *Chem. Eng. Sci.*, **31**, 1101 (1976).

Dow Chemical Co., Bulletin "Alpha-Methyl Styrene Monomer" (1955).

Dwivedi, P. N., and S. N. Upadhyay, "Particle-Fluid Mass Transfer in Fixed and Fluidized Beds," *Ind. Eng. Chem. Process Design Develop.*, **16**, 157 (1977).

Germain, A. H., A. G. Lefebvre, and G. A. L'Homme, "Experimental Study of a Catalytic Trickle-Bed Reactor," *Chem. Reac. Eng. II*, ACS Monograph Ser. No. 133, p. 164 (1974).

Goto, S., and J. M. Smith, "Trickle-Bed Reactor Performance, Part I. Holdup and Mass Transfer Effects," *AIChE J.*, **21**, 706 (1975).

Herskowitz, M., and J. M. Smith, "Liquid Distribution in Trickle-Bed Reactors, Part I: Flow Measurements," *ibid.*, **24**, 439 (1978).

Herskowitz, M., "The Performance of Trickle-Bed Reactors," Ph.D. thesis, Univ. Calif., Davis (1978).

———, S. Morita, and J. M. Smith, "Solubility of Hydrogen in α-Methyl Styrene," *J. Chem. Eng. Data*, **23**, 227 (1978).

Hildebrand, R. B., *Advanced Calculus for Applications*, 2 ed., Prentice-Hall, Englewood Cliffs, N.J. (1976).

Morita, S., and J. M. Smith, "Mass Transfer and Contacting Efficiency in Trickle-Bed Reactors," *Ind. Eng. Chem. Fundamentals*, **17**, 113 (1978).

Niiyama, Hiroo, and J. M. Smith, "Adsorption of Nitric Oxide in Aqueous Slurries of Activated Carbon: Transport Rates by Moment Analysis of Dynamic Data," *AIChE J.*, **22**, 961 (1976).

Reid, R. C., J. M. Prausnitz, and T. K. Sherwood, *The Properties of Gases and Liquids*, 3 ed., McGraw-Hill, New York (1977).

Satterfield, C. N., "Trickle-Bed Reactors," *AIChE J.*, **21**, 209 (1975).

———, and F. Ozel, "Direct Solid Catalyzed Reaction of a Vapor in an Apparently Completely Wetted Trickle-Bed Reactor," *ibid.*, **19**, 1259 (1973).

Satterfield, C. N., A. A. Pelossof, and T. K. Sherwood, "Mass Transfer Limitations in a Trickle-Bed Reactor," *ibid.*, **15**, 226 (1969).

Satterfield, C. N., Y. H. Ma, and T. K. Sherwood, "The Effectiveness Factor in a Liquid-Filled Porous Catalyst," *Ind. Chem. Eng. Symp. Ser. No. 28*, 22 (1968).

Schwartz, J. G., E. Weger, and M. P. Dudukovic, "A New Tracer Method for Determination of Liquid-Solid Contacting Efficiency in Trickle-Bed Reactors," *AIChE J.*, **22**, 894 (1976).

Sedriks, W., and C. N. Kenney, "Partial Wetting Trickle-Bed Reactors: the Reduction of Crotonaldehyde over a Palladium Catalyst," *Chem. Eng. Sci.*, **28**, 559 (1973).

Sporka, K., J. Hanika, V. Ruzicka, and M. Halousek, "Diffusion of Gases in Liquids, III. Diffusion Coefficients of Hydrogen in Organic Solvents," *Colln. Czech. Chem. Commun.*, **36**, 213 (1971).

Sovova, H., "A Correlation of Diffusivities of Gases in Liquids," *ibid.*, **41**, 3715 (1976).

Whitaker, S., "Forced Convection Heat Transfer Correlations for Flow in Pipes, Past Flat Plates, Single Cylinders, Single Spheres, and for Flow in Packed Bed and Tube Bundles," *AIChE J.*, **18**, 361 (1972).

APPENDIX

The expression for the effectiveness factor, Equation (27), using the solution to Equation (18) for the special case of $f = 5/6$, is given by

$$\eta_o = \sum_m^\infty \sum_n^\infty \left\{ \frac{2 \operatorname{Sin}^2 \lambda_n \operatorname{Sin}^2 \kappa_m / (\lambda_n^2 \kappa_m^2 b_{mn})}{(\coth b_{mn} + b_{mn}/\alpha_{gLs}) \left[a_m^2 + (1 - a_m^2) \left(\frac{1}{2} + \frac{1}{4\kappa_m} \sin 2\kappa_m \right) \right] \left(\frac{1}{2} + \frac{1}{4\lambda_n} \sin 2\lambda_n \right)} \right.$$

$$+ \frac{\operatorname{Sin}^2 \lambda_n \operatorname{Sin}^2 \lambda_m / (\lambda_m^2 \lambda_n^2 g_{mn})}{\left(\frac{1}{2} + \frac{1}{4\lambda_n} \operatorname{Sin} 2\lambda_n \right) \left(\frac{1}{2} + \frac{1}{4\lambda_m} \operatorname{Sin} 2\lambda_m \right)} \left[\frac{1}{l_{mn} + g_{mn}/\alpha_{gLs} + (1 + l_{mn} g_{mn}/\alpha_{gLs}) \coth g_{mn}} \right.$$

$$\left. \left. + \frac{1}{d_{mn} + g_{mn}/\alpha_{gs} + (1 + d_{mn} g_{mn}/\alpha_{gs}) \coth g_{mn}} \right] \right\} \quad \text{(A1)}$$

where

$$\frac{1}{\alpha_{gLs}} = \frac{1}{\alpha_{gL}} + \frac{1}{\alpha_{Ls}} \quad \text{(A2)}$$

$$b_{mn} = (\lambda_n^2 + \kappa_m^2 + \phi_c^2)^{1/2} \quad \text{(A3)}$$

$$g_{mn} = (\lambda_n^2 + \lambda_m^2 + \phi_c^2)^{1/2} \quad \text{(A4)}$$

$$d_{mn} = \frac{g_{mn} \tanh g_{mn} + \alpha_{gLs}}{g_{mn} + \alpha_{gLs} \tanh g_{mn}} \quad \text{(A5)}$$

$$l_{mn} = \frac{\alpha_{gs} + g_{mn} \tanh g_{mn}}{\alpha_{gs} \tanh g_{mn} + g_{mn}} \quad \text{(A6)}$$

and λ_n and κ_m are the roots of

$$\lambda_n \tan \lambda_n = \alpha_{gLs}; \quad n = 1, 2, \cdots \quad \text{(A7)}$$

$$\left(\kappa_m + \frac{\alpha_{gLs}}{\alpha_{gs}} \right) \tan^2 \kappa_m - 2 \left(\alpha_{gLs} - \frac{\kappa_m^2}{\alpha_{gs}} \right) \tan \kappa_m - \left(\frac{\alpha_{gLs}}{\alpha_{gs}} + 1 \right) \kappa_m = 0; \quad m = 1, 2, \cdots \quad \text{(A8)}$$

Similar relations were obtained for the cases $f = 1/6$, 2/6, 3/6, 4/6 and can be found in Herskowitz (1978).

Manuscript received June 2, 1978; revision received October 23, and accepted November 13, 1978.

Interfacial Effects in the Displacement of Residual Oil by Foam

A qualitative theory is developed to explain the roles of surface tension and the two surface viscosities in the displacement of foams through porous media. There is a critical value of the surface tension above which a foam cannot be displaced under a given pressure gradient. The displacement efficiency of a foam can be raised by increasing the surface tension to only slightly less than this critical value, by increasing the viscosity of the aqueous surfactant solution from which the foam is formed and by increasing the surface viscosities. These predictions are in agreement with available experimental data.

JOHN C. SLATTERY

Department of Chemical Engineering
Northwestern University
Evanston, Illinois 60201

SCOPE

Petroleum is found in the microscopic pores of sedimentary rocks such as sandstones and limestones. Not all of the pores are filled with petroleum. Some of the pores contain water or brine that is saturated with minerals from the local rock structure.

In the primary stage of production, oil and brine are driven into a well from the surrounding rock by the relatively large difference between the initial field pressure and the pressure in the well. In the secondary stage of conventional production, water or steam is pumped into a selected pattern of wells in a field forcing a portion of the oil toward the production wells.

A number of tertiary recovery techniques have been proposed (Geffen, 1973). The one with which we shall concern ourselves here is a gas drive, in which the residual oil is displaced by a gas. The most favorable conditions for displacement would occur if the gas were miscible with the oil at the reservoir temperature and pressure. But even if the gas is not miscible with the oil, it will still be soluble in the oil under reservoir conditions. This can result in a reduced viscosity of the oil, a reduced density of the oil (the volume of the oil would be increased), and possibly a reduced gas-oil interfacial tension. Any combination of these factors can enhance the displacement of residual oil.

A major disadvantage of a gas drive is that the mobility of the gas (the ratio of the relative permeability of the gas to its viscosity) is much larger than the mobility of the oil. This results in an unstable displacement, with the gas fingering ahead through the oil and water and bypassing the majority of it.

0001-1541-79-2159-0283-$00.85.